http://dx.doi.org/10.5012/bkcs.2014.35.4.1110

Fabrication and Photocatalytic Properties of Visible Light Responsive Cuprous Oxide Cubes

Jiudong Lin, Feifei Tao,* Congcong Sheng, Jianwei Li, and Xiaoding Yu

Department of Chemistry and Chemical Engineering, Shaoxing University, Shaoxing 312000, P.R. China
**E-mail: fingal.tao@gmail.com*
Received September 25, 2013, Accepted December 20, 2013

The cuprous oxide cubes with the special porous surface constructed by nano-prisms have been successfully fabricated by a solvothermal method. The template-free method is simple and facile without any surfactant. The X-ray powder diffraction (XRD) pattern suggests that the as-prepared product is the pure primitive cubic Cu_2O. The effects of the experimental parameters, such as the reaction temperature, reaction time and the concentration of sodium acetate anhydrous, on the morphologies of the products were investigated in detail by the scanning electron microscopy (SEM). Based on the time-dependent experiments, the possible formation mechanism was proposed. Using photocatalytic degrading reactive dyes as the model reaction and xenon lamp to simulate sunlight, the Cu_2O cubes with the porous surface might possess higher photocatalytic activity than those of the commercial Cu_2O powder in the visible-light region, indicating the excellent photocatalytic performance.

Key Words : Cuprous oxide, Visible light, Photocatalysis

Introduction

In recent years, the photocatalytic degradation of organic pollutants in wastewater has been the research hotspot in the field of environmental pollution control. Semiconductor-based photocatalysis has attracted much attention due to its application in degrading organic contaminants from wastewater with solar energy in recent years.[1-3] Among them, TiO_2 has been deemed to be an ideal photocatalyst in water splitting and treating organic pollutants in water, due to its non-toxic, good stability and high photocatalytic properties.[4-6] However, the wide band gap semiconductor characteristics (E_g > 3.2 eV) of TiO_2 required UV light (λ < 387 nm) as an excitation resource, which greatly limits further practical applications of this materials in the visible-light region (λ > 400 nm). Therefore, in order to efficiently utilize the solar energy, it is necessary to explore the new visible light photocatalysts with high activity.

Semiconductor transition-metal oxides have been of much interest because of their excellent properties and wide-range potential applications. In particular, cuprous oxide (Cu_2O), as an important p-type semiconductor with a band gap of 2.17 eV, is a promising material with potential applications in solar energy conversion,[7] catalysis,[8] and sensing.[9] Recently, many efforts have been devoted to the synthesis of Cu_2O micro- and nano-materials with modulated morphologies and architectures.[10-12] Morphology-controlled synthesis of various Cu_2O particles, such as nanocrystals,[13] nanowires,[14] nanorod,[15] microspheres,[16] hollow spheres[17] and cubes,[18-20] has been realized by various methods. Although considerable progress has been made in the synthesis of Cu_2O particles, there are few researches on the preparation of the Cu_2O cubes with the porous surface constructed by nano-prisms using the template-free method. Therefore, developing a facile and template-free method to prepare the porous Cu_2O cubes is of scientific and practical importance.

In this paper, cuprous oxide cubes with the porous surface constructed by nano-prisms have been successfully fabricated by the solvothermal method using $CuCl_2{\cdot}2H_2O$ as the copper source, glucose as the reducing agent and anhydrous sodium acetate as the additive, ethanol-water as mixed solvent. The template-free method is simple, facile and effective without any surfactant. Using reactive dye light catalytic degradation as the probe response and xenon lamp to simulate sunlight, the Cu_2O cubes exhibit higher photocatalytic activity than those of the commercial Cu_2O powder under visible light irradiation, indicating the prominent photocatalytic performance.

Experimental

Reagents. Copper chloride dihydrate ($CuCl_2{\cdot}2H_2O$), anhydrous sodium acetate (NaAc), anhydrous glucose, cuprous oxide, hydrogen peroxide, and all other regents are analytical grade. Reactive dyes, such as reactive red R-4BD (RR), reactive brilliant yellow R-4GLN (RBY), reactive dark blue R-2GLN (RDB) and reactive black R-2BR (RB), were purchased from Zhejiang Runtu Co., Ltd, China. The water used in the whole experiments is the distilled water.

Preparation of Cu_2O Cubes. 0.34 g of $CuCl_2{\cdot}2H_2O$ was dissolved in 10 mL of anhydrous ethanol to form solution A. 0.50 g of NaAc and 0.40 g of anhydrous glucose were dissolved in 10 mL of distilled water to form solution B. Then, solution A was slowly dropped into solution B under stirring treatment. After that, the mixture was filled into a dried autoclave (22 mL volume) lined with polytetrafluoro-

ethylene. The autoclave was sealed and placed in an oven, and then kept at 120 °C for 12 h. After completion of the reaction, the autoclave was naturally cooled to room temperature. Through centrifugation the solid powder was collected and washed with distilled water and ethanol more than five times, and then placed in the oven of 60 °C for 3 h and dried to obtain the product.

Characterization. The morphologies and structures of the products were characterized by scanning electron microscopy (SEM, JEOL JSM-6360LV, 20 kV) and X-ray diffraction (XRD, Empyrean, Netherlands PANalytical Inc.), by using Cu Kα radiation with the wavelength of 1.5406 Å. Nitrogen sorption isotherms of Cu_2O cubes were obtained from a Micromeritics TriStar 3020 instrument.

Photocatalytic Decomposition of Reactive Dyes. 5 mg as-prepared product was placed in 10 mL of 20 $mg \cdot L^{-1}$ of the reactive dye solution (reactive red R-4BD, reactive brilliant yellow R-4GLN, reactive dark blue R-2GLN and reactive black R-2BR), and then added 0.05 mL of 30 wt % hydrogen peroxide solution. After that, the mixture was placed into the dark place for 30 min to make the photocatalyst reach the adsorption/desorption equilibrium. Using a 250 W xenon lamp to simulate sunlight, the reactive dye solution was irradiated for some time. After irradiation, the mixture was centrifuged and the clear solution was checked by UV-visible spectrometer (HP8453, U.S. Agilent Company) to measure the concentration of the reactive dye in the solution. The decolorization rate (η) is used to denote the degradation extent of the reactive dye.

$$\eta = [(A_0 - A)/A_0] \times 100\%$$

Where, A_0 and A are the absorbance of reactive dye before dark adsorption and after the illumination, respectively.

Results and Discussion

Characterization of the Cu_2O Cubes. The morphology of the as-prepared sample was investigated by scanning electron microscopy (SEM) technology. Figure 1(a) shows that the cubes have a size of about 30 μm with the good dispersion. In Figure 1(b) a further enlarged SEM image of a single cube exhibits that the surface of the cubes is constructed by many irregular nano-prisms. The interwoven nano-prisms are attached to the growth surface of the cubes, so that the surface becomes rough and has porous structures, leading to many actives sites and high catalytic activities. Figure 1(c) shows the X-ray diffraction (XRD) pattern of the as-prepared sample. The diffraction peaks at 29.5°, 36.3°, 42.3°, 52.3°, 61.3°, 69.4°, 73.4° and 77.3° can be indexed to the primitive cubic phase Cu_2O (110), (111), (200), (211), (220), (310), (311) and (222) crystal faces, in good agreement with Cu_2O standard diagram (JCPDS No. 78-2076). The diffraction peaks of the Cu and CuO are not found, indicating that the as-prepared product is pure Cu_2O.

The above SEM images of Cu_2O cubes clearly show the rough and porous surface structures. Nitrogen adsorption-desorption isotherm measurement was performed to investigate the adsorption property. Figure 2 presents the nitrogen absorption and desorption isotherms for the Cu_2O cubes. The BET surface area of the Cu_2O cubes is only 0.70 $m^2 \cdot g^{-1}$, which is so little likely due to the larger micrometer size of the Cu_2O cubes (Figure 1(a)). The pore diameter distribution of the product was measured by the Barret-Joyner-Halenda

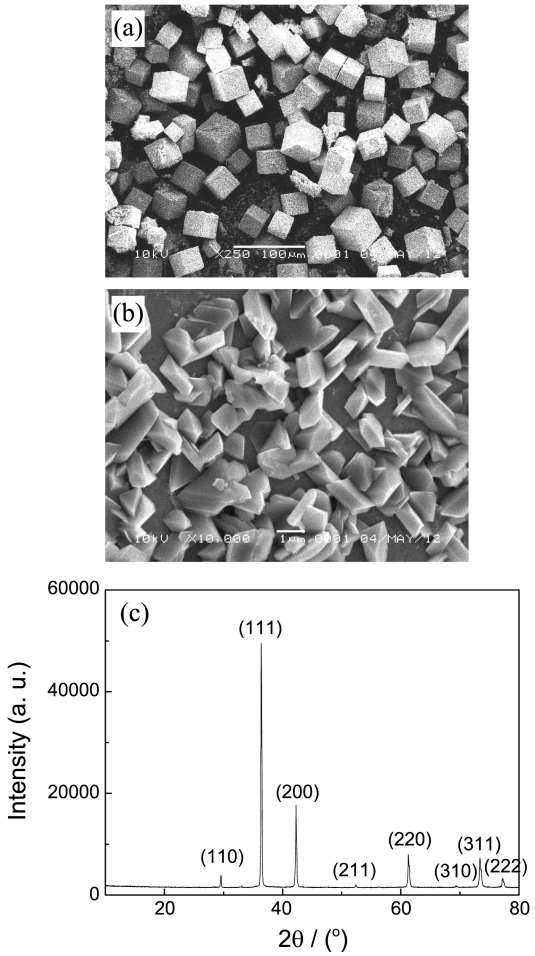

Figure 1. SEM images (a and b) and XRD pattern (c) of the as-prepared product.

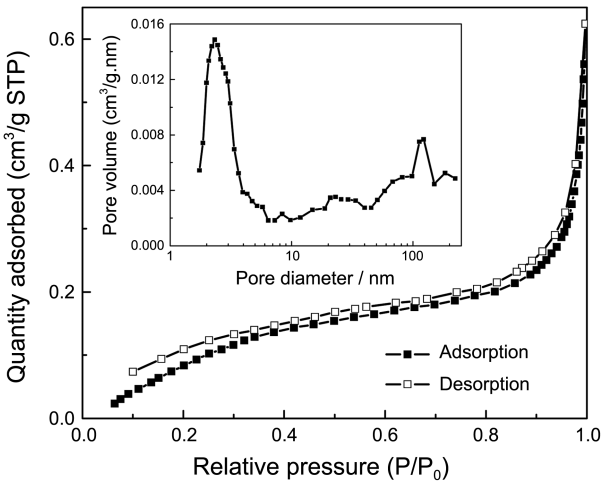

Figure 2. N_2 adsorption and desorption isotherms and pore size distributions (inset) of Cu_2O cubes.

(BJH) method and is shown in the inset of Figure 2. The pore size distribution calculated by the adsorption branch is divided into two parts, the mesoporous size from the sample itself is about 2.3 nm and the microporous size from the disordered aggregation of nano-prisms is in the range of 20-120 nm. The Cu_2O cubes with nano-prisms and porous characteristics will potentially exhibit superior performance in the visible-light photocatalysis.

Growth Mechanism of Cu_2O Cubes. To get an insight into the formation mechanism of Cu_2O cubes with the porous cube surface, the effects of the experimental parameters on the formation of Cu_2O cubes were investigated in detail. It is found that the reaction temperature played a crucial role in the formation of the products, as shown in Figure 3. At the lower reaction temperature than 100 °C, there is not any product obtained. When the reaction temperature is 100 °C, only a very small amount of red-brown precipitate can be collected and the products are composed of the uneven cubes with the poor dispersion (Figure 3(a)). The enlarged SEM image of the single cube indicates that the surface of the cube is not very smooth, as shown in Figure 3(b). At the reaction temperature of 120 °C, the obtained cubes with good dispersion have a uniform size and rough surface constructed by many irregular nano-prisms (Figure 1(a) and (b)). When the reaction temperature continues to rise up to 140 °C (Figure 3(c) and (d)), the cubes with good dispersion have the uniform size of about 30 μm, which does not change significantly with the increasing reaction temperature. However, one or more breaks are found on each surface of the cube near the center position, indicating that the structural integrity is destroyed. As the reaction temperature is further increased to 160 °C (Figure 3(e) and (f)), the cubes gradually disappear and there is a small amount of microrods found in the as-prepared product, in addition to the irregular blocks. It is suggested that the dissolution-recrystallization process can proceed with the increasing reaction temperature. In order to obtain the uniform cubes with the porous surface, the reaction temperature of 120 °C is used to prepare the Cu_2O cubes with the good dispersion.

Therefore, the reaction temperature plays an important role on morphology of the product. When the reaction temperature is higher than 100 °C, the cubes are fabricated. As the temperature increases, the cubes will gradually become uniform in the size and have the rougher surface. When the reaction temperature is 120 °C, the cubes with a good dispersion are fabricated and the size is about 30 μm. With the increasing reaction temperature, the cubes gradually dissolve and some breaks appear on the cubic surface. When the reaction temperature exceeds to 160 °C, the cubes are completely destroyed and the irregular particles and microrods are obtained.

In order to further make clear the formation of Cu_2O cubes, the effect of reaction time on the morphology of the product was investigated, as shown in Figure 4. It is found that when the reaction time is 4 h, only a very small amount of red-brown precipitate is obtained. Figure 4(a) and (b) show that at this time the cubes have the different size and

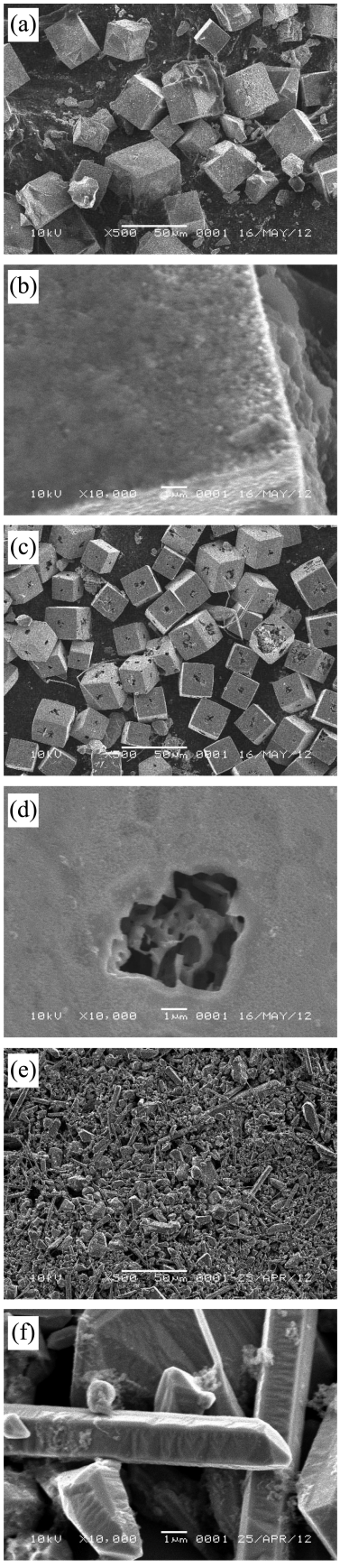

Figure 3. SEM images of the as-prepared products at the different reaction temperatures, (a and b) 100 °C, (c and d) 140 °C, (e and f) 160 °C.

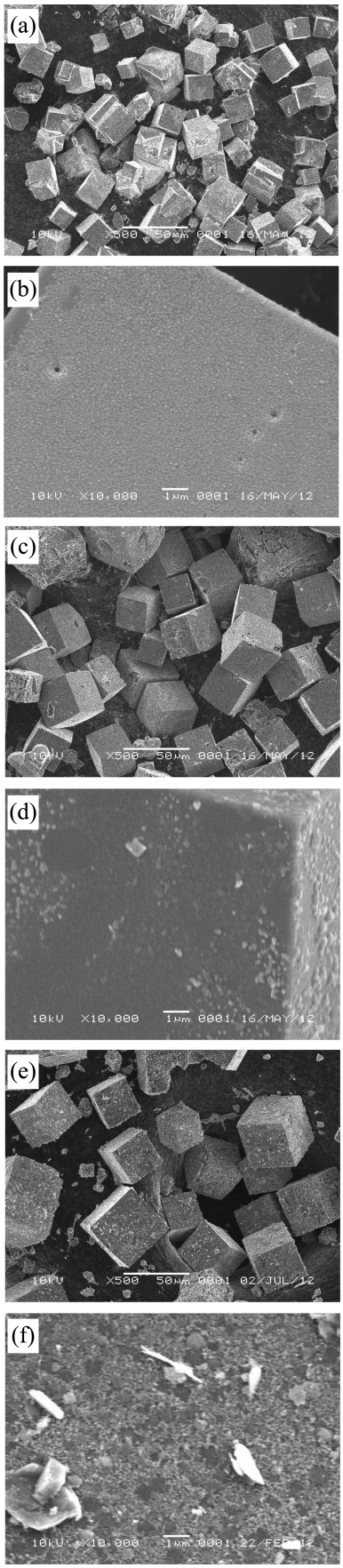

Figure 4. SEM images of the as-prepared products at the different reaction times, (a and b) 4 h, (c and d) 7 h, (e and f) 8 h.

smooth surface. Among them, a number of cubes intertwine each other, leading to poor dispersion. When the reaction time is prolonged to 7 h in Figure 4(c) and (d), the size of the cube further increases with markedly improved dispersion and only a small number of cubes are intertwined. In addition, the surface of the cubes becomes rough, and a small amount of tiny particles begin to grow on its surface. When the reaction time extends to 8 h in Figure 4(e) and (f), the dispersion of the cubes is developed with different sizes. When the reaction time is 12 h in Figure 1(a) and (b), the cubes have a good dispersion and uniform size. The further growth of small particles on the surface of the cubes brings about the formation of many irregular nano-prisms. Therefore, the formation of Cu_2O cubes experiences the nucleation-regrowth process. That is to say, using the protuberance of the cube surface as the second growth point, the remaining Cu^{2+} ions in the reaction solution continue to make nucleus and grow up on the cubic surface, which leads to the unique cubic surface composed of many irregular nano-prisms.

Based on the above analysis, only when the reaction time is 4 h, the cubes are obtained. And with the increasing reaction time, the dispersion and the uniformity of the cubes are improved, while the surface of the cubes becomes rougher.

In addition, the effect of the added amount of NaAc on the morphology of the product is investigated in Figure 5. When

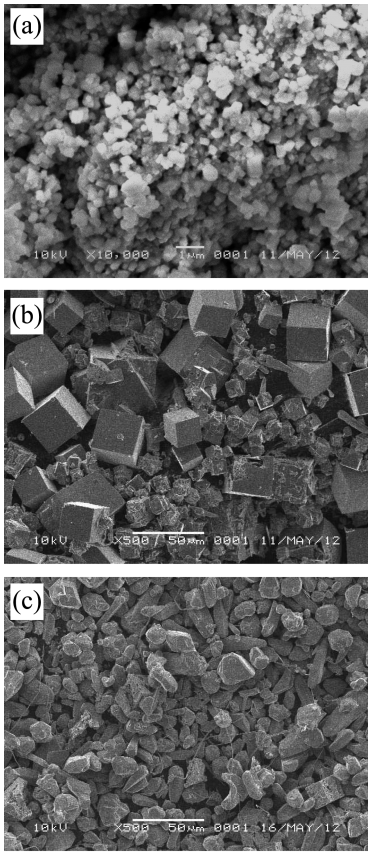

Figure 5. SEM images of the as-prepared products added by the different concentration of sodium acetate anhydrous, (a) 0.25 g, (b), 0.75 g, (c) 1.00 g.

0.25 g of anhydrous sodium acetate is added (Figure 5(a)), the sphere-like particles with the size of about 300 nm are obtained. When the added amount increases to 0.50 g (Figure 1(a), and (b)), the cubes with the porous surface are formed and have the size of about 30 μm. As the amount raises to 0.75 g (Figure 5(b)), the cubes gradually become irregular and have the poor dispersion. When the amount of NaAc further increased up to 1.00 g (Figure 5(c)), there are no cubes but the massive particles with irregular size.

Therefore, the added amount of NaAc plays an important role on the formation of cubes. The possible reason for this phenomenon is the pH value of the reaction system from the hydrolyzing of anhydrous sodium acetate. The more addition of NaAc makes the stronger alkaline of the reaction solution. Only when added amount of NaAc is 0.50 g, could we obtain a uniform cubic Cu_2O with the good dispersion.

In summary, only when 0.50 g of NaAc is added in the reaction system, the cubes with good dispersion and relatively uniform size are fabricated at the reaction temperature of 120 °C for 12 h. According to crystal growth kinetics, the rate of crystal growth at the different crystal face makes an important effect on the morphology of the product. The crystal face with smaller growth rate will eventually turn into the exposed surface, while the crystal surface with faster growth rate will disappear in the crystal growth. According to the XRD pattern (Figure 1(c)), the Cu_2O cubes have a primitive cubic crystal structure. Due to the fast growth rate of the crystal face (111), the crystal face (100) is exposed, leading to the cubic structures of Cu_2O materials.

Photocatalytic Activity of Cu_2O Cubes. UV-vis spectra was applied to demonstrate the photocatalytic degradation activity of reactive red R-4BD (RR) in aqueous solution under xenon lamp irradiation. The characteristic absorption peak of RR at 519 nm was used as a monitored parameter during the photocatalytic degradation process. Figure 6 shows the effect of the irradiation time on the decolorization rate of RR at room temperature. It is found that when the photocatalytic degradation is less than 40 min, the decolorization rate of RR increases significantly with extended illumination time, but does not have a linear relationship with the irradiation time. After 40-min illumination, about 90% of the RR was degraded. After that, the decolorization rate changes slowly with the irradiation time. When the illumination is 120 min, the RR has been almost completely degraded and the decolorization rate reaches 98.8%. For comparison, the photocatalytic degradation of RR was carried out in the presence of the commercial Cu_2O powder, as shown in Figure 6. At the same experimental conditions, after 120-min irradiation, only 33.3% of the RR was degraded. It is expected that the Cu_2O cubes with the porous surface will exhibit higher photocatalytic activity under xenon lamp irradiation. And in order to ensure the high decolorization rate of RR, the illumination time of 120 min is more appropriate.

Figure 7 shows the effect of the amount of the Cu_2O cubes on the degradation rate of RR. The Cu_2O cubes with different amount are placed in a 10 mL of 20 $mg \cdot L^{-1}$ RR solution. After 30 min of dark adsorption, the mixture is placed into the light reactor and irradiated for 120 min. It is found that the decolorization rate first significantly goes up and then decreases with the increasing amount of the Cu_2O cubes. When the solid-liquid ratio is 0.2 $g \cdot L^{-1}$, the decolorization rate reaches 93.2%. At the solid-liquid rate of 0.5 $g \cdot L^{-1}$, the RR is almost degraded and the decolorization rate goes up to 98.8%. When the Cu_2O cubes continue to be added in the reaction solution, 97.1% of RR is degraded at the solid-liquid ratio of 1.2 $g \cdot L^{-1}$. It is the possible reason that with the increasing amount of the Cu_2O cubes, the catalyst would interweave together, leading to the less chance to contact with H_2O_2. The low number of ·OH active groups makes the low degradation rate of RR. In addition, at the large amount of Cu_2O cubes, the formed suspension of the RR and the catalyst under stirring leads to the strong light scattering, the low effective light intensity, the decreased activity of the catalyst to absorb the light irradiation, and the low quantum yield. Thus, the solid-liquid ratio of 0.5 $g \cdot L^{-1}$ of catalyst is the best adding amount of Cu_2O cubes.

In order to investigate the effect of the pH value on the photocatalytic degradation rate, the hydrochloric acid solu-

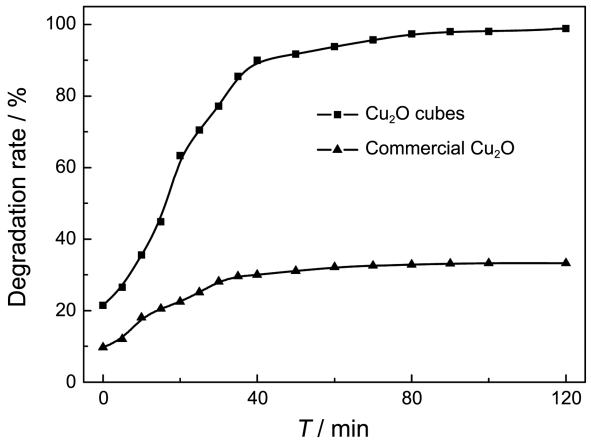

Figure 6. Effect of irradiation time on the degradation rate of reactive red R-4BD.

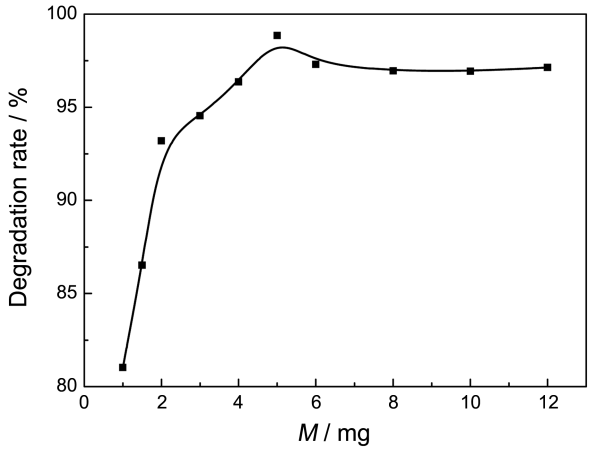

Figure 7. Effect of the mass of Cu_2O cubes on the degradation rate of reactive red R-4BD.

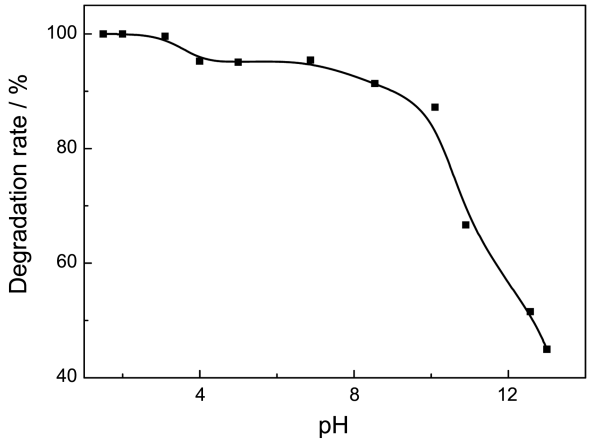

Figure 8. Effect of pH value on the degradation rate of reactive red R-4BD.

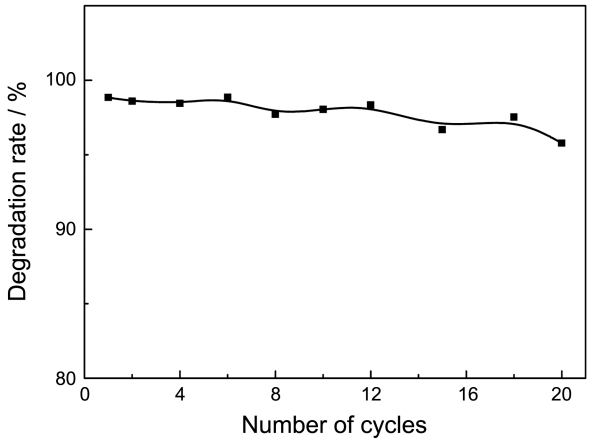

Figure 10. Effect of number of cycles on the degradation rate of reactive red R-4BD.

tion and sodium hydroxide solution are used to adjust the pH value, and the experimental data are shown in Figure 8. It is found that the pH value of the solution has a significant effect on the decolorization rate of the RR. When the pH value is less than 4, the degradation rate of the RR is very high and close to 100%. When the pH value is under weak acidic environment and neutral conditions at the range of 4 to 7, the decolorization rate can also reach 95%. When the pH value is more than 10, the decolorization rate decreases significantly with the increasing pH value and is less than 90%. The reason for this phenomenon may be due to an acidic environment, in which the hydrogen ion neutralizes the hydroxide anion to promote the reaction, thereby creating a large number of ·OH active groups to make the photocatalytic reaction complete. While the alkaline conditions inhibit the generation of ·OH active groups, leading to the low decolorization rate. The experimental data show that the Cu_2O cubes in a wide pH range of 0-7 can effectively make the RR degrade. From a more economical and convenient view, the neutral environment can be selected as the optimum reaction conditions.

In order to investigate the universality of photocatalytic activity of Cu_2O cubes, the photocatalytic performance for various reactive dyes in the presence of the Cu_2O cubes or commercial Cu_2O powder is shown in Figure 9. At the similar experimental conditions, the degradation rates for various reactive dyes differ from each other, but in the presence of the Cu_2O cubes they are obviously higher than those with the assistance of the commercial Cu_2O powder. Among them, in the presence of the Cu_2O cubes the degradation of RR is best

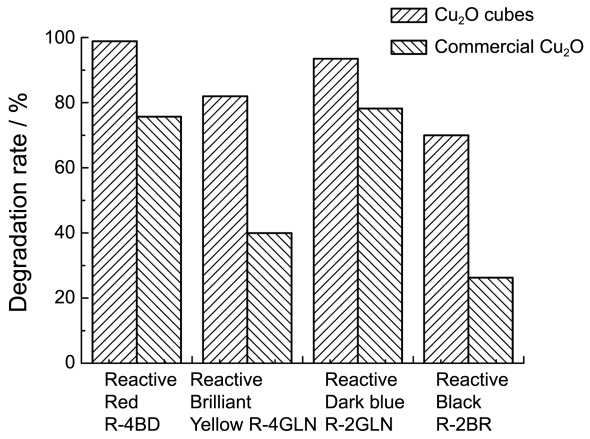

Figure 9. The degradation rate of various reactive dyes under the assistance of Cu_2O cubes and commercial Cu_2O powder.

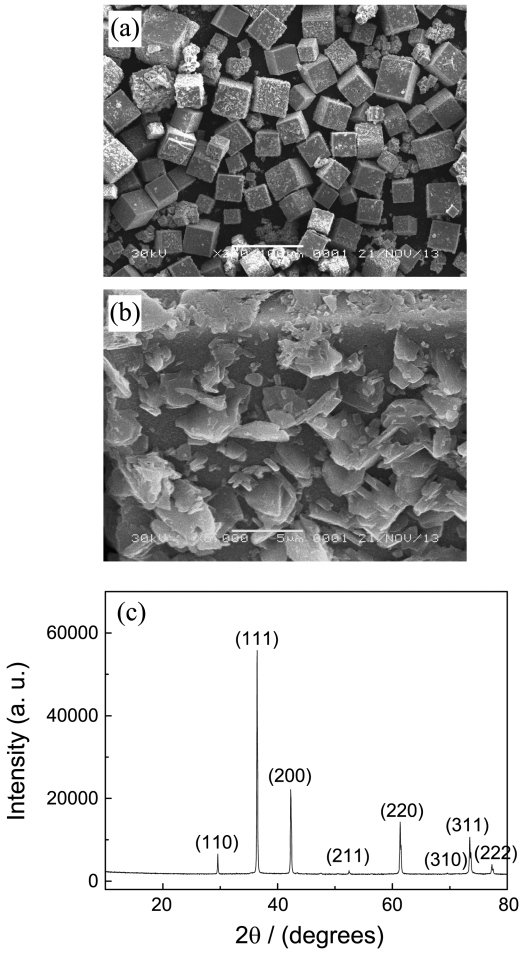

Figure 11. SEM images (a and b) and XRD pattern (c) of the product after the photocatalytic reaction.

and reaches 98.8%, while for the RB the degradation rate is poorest and only 70.0%. Compared with those of other reactive dyes, this value is low, but it can reach 2.7 times as big as that of the commercial Cu_2O powder. Based on the comparison with the commercial Cu_2O powder, the Cu_2O cubes exhibit the prominent photocatalytic properties for various reactive dyes, indicating that the Cu_2O cubes with the porous surface constructed by nano-prisms have better universality and potential applications as visible light photocatalyst.

To evaluate the reproducibility and stability of the Cu_2O cubes, the effect of reaction times on degradation rates of the RR is shown in Figure 10. It is found that after 20 cyles, the degradation rate is still more than 95%, indicating the good stability of the Cu_2O cubes. To further make clear the effect of photocatalytic reaction on morphology and crystal structures of Cu_2O cubes, the SEM images and XRD pattern of the used Cu_2O cubes after photocatalytic reaction are shown in Figure 11. The SEM image in Figure 11(a) indicates that the cubic structure of the reacted Cu_2O sample has been hardly changed by the photocatalytic reaction. Based on the further enlarged SEM image in Figure 11(b), it is found that the interwoven nano-prisms still exist on the cubic surface and their further development leads to the aggregation of nano-prisms and the formation of the larger prism-like structures. However, compared with the unreacted Cu_2O, the crystal structure of the reacted Cu_2O cubes has been hardly changed by the photocatalytic reaction (Figure 11(c)). It is indicated that the good stability of the morphology and crystal structures could facilitate the photocatalytic reaction.

Conclusion

The cuprous oxide cubes with the special surface composed of nano-prisms have been successfully fabricated by the solvothermal method. The template- and surfactant-free method is simple, effective, controllable and reproducible for the preparation of the Cu_2O cubes with the uniform size and good dispersion. Through SEM characterization, the effects of the reaction parameters, such as reaction temperature, reaction time and the amount of NaAc, on the morphologies of the products have been investigated in detail. It is suggested that under the assistance of 0.50 g NaAc, the uniform Cu_2O cubes with unique structures and high purity can be well fabricated at 120 ^oC for 12 h. Based on the time-dependent experiments, the possible formation mechanism of the Cu_2O cubes with the special structures is proposed. Taking the photocatalytic degradation of reactive dyes as the probe reactions, the photocatalytic properties of the Cu_2O cubes are investigated. Compared with the commercial Cu_2O powder, the Cu_2O cubes with the porous surface constructed by nano-prisms exhibit the higher degradation rates for various reactive dyes, indicating that the Cu_2O cubes have the good photocatalytic activities for the removal of reactive dyes as the visible light photocatalyst.

Acknowledgments. We thank the financial support from the National Natural Science Foundation of China (Nos 51372154 and 20901051), Zhejiang Provincial Natural Science Foundation of China (No. LY12B01007), and Zhejiang Provincial Science Technolgy Plan of China (No. 2013C33010).

References

1. Tanaka, A.; Fuku, K.; Nishi, T.; Hashimoto, K.; Kominami, H. *J. Phys. Chem. C* **2013**, *117*, 16983.
2. Yang, M.-Q.; Weng, B.; Xu, Y.-J. *Langmuir* **2013**, *29*, 10549.
3. Lee, G.-J.; Manivel, A.; Batalova, V.; Mokrousov, G.; Masten, S.; Wu, J. *Ind. Eng. Chem. Res.* **2013**, *52*, 11904.
4. Wang, X.-J.; Li, F.-T.; Liu, J.-X.; Kou, C.-G.; Zhao, Y.; Hao, Y.-J.; Zhao, D. *Energy Fuels* **2012**, *26*, 6777.
5. Guo, Q.; Xu, C.; Ren, Z.; Yang, W.; Ma, Z.; Dai, D.; Fan, H.; Minton, T. K.; Yang, X. *J. Am. Chem. Soc.* **2012**, *134*, 13366.
6. El-Roz, M.; Kus, M.; Cool, P.; Thibault-Starzyk, F. *J. Phys. Chem. C* **2012**, *116*, 13252.
7. Cao, D.; Wang, C.; Zheng, F.; Dong, W.; Fang, L.; Shen, M. *Nano Lett.* **2012**, *12*, 2803.
8. Zhang, Y.; Deng, B.; Zhang, T.; Gao, D.; Xu, A.-W. *J. Phys. Chem. C* **2010**, *114*, 5073.
9. Zhang, H.; Zhu, Q.; Zhang, Y.; Wang, Y.; Zhao, L.; Yu, B. *Adv. Funct. Mater.* **2007**, *17*, 2766.
10. Paolella, A.; Brescia, R.; Prato, M.; Povia, M.; Marras, S.; Trizio, L. D.; Falqui, A.; Manna, L.; George, C. *ACS Appl. Mater. Interfaces* **2013**, *5*, 2745.
11. Fan, W.; Wang, X.; Cui, M.; Zhang, D.; Zhang, Y.; Yu, T.; Guo, L. *Environ. Sci. Technol.* **2012**, *46*, 10255.
12. Deng, S.; Tjoa, V.; Fan, H. M.; Tan, H. R.; Sayle, D. C.; Olivo, M.; Mhaisalkar, S.; Wei, J.; Sow, C. H. *J. Am. Chem. Soc.* **2012**, *134*, 4905.
13. Luo, F.; Wu, D.; Gao, L.; Lian, S.; Wang, E.; Kang, Z.; Lan, Y.; Xu, L. *J. Cryst. Growth* **2005**, *285*, 534.
14. Grez, P.; Herrera, F.; Riveros, G.; Henríquez, R.; Ramírez, A.; Muñoz, E.; Dalchiele, E. A.; Celedón, C.; Schrebler, R. *Mater. Lett.* **2013**, *92*, 413.
15. Ju, H.; Lee, J. K.; Lee, J.; Lee, J. *Curr. Appl. Phys.* **2012**, *12*, 60.
16. Zhang, Z.; Che, H.; Wang, Y.; Gao, J.; Zhao, L.; She, X.; Sun, J.; Gunawan, P.; Zhong, Z.; Su, F. *Ind. Eng. Chem. Res.* **2012**, *51*, 1264.
17. Sui, Y.; Zhang, Y.; Fu, W.; Yang, H.; Zhao, Q.; Sun, P.; Ma, D.; Yuan, M.; Li, Y.; Zou, G. *J. Cryst. Growth* **2009**, *311*, 2285.
18. Miao, W.; Liu, H.; Zhang, Z.; Chen, J. *Solid State Sci.* **2008**, *10*, 1322.
19. Zhu, J.; Bi, H.; Wang, Y.; Wang, X.; Yang, X.; Lu, L. *Mater. Lett.* **2008**, *62*, 2081.
20. Uhm, Y. R.; Park, J. H.; Kim, W. W.; Lee, M. K.; Rhee, C. K. *Mater. Sci. Eng. A* **2007**, *449-451*, 817.